Roles of UGT, P450, and Gut Microbiota in the Metabolism of Epacadostat in Humans

Jason Boer, Ruth Young-Sciame, Fiona Lee, Kevin J. Bowman, Xiaoqing Yang, Jack G. Shi, Frank M. Nedza, William Frietze, Laurine Galya, Andrew P. Combs, Swamy Yeleswaram, and Sharon Diamond

Incyte Corporation, Wilmington, Delaware

Received March 31, 2016; accepted July 20, 2016

ABSTRACT

Epacadostat (EPA, INCB024360) is a first-in-class, orally active, investigational drug targeting the enzyme indoleamine 2,3-dioxygenase 1 (IDO1). In Phase I studies, EPA has demonstrated promising clinical activity when used in combination with checkpoint modulators. When the metabolism of EPA was investigated in humans, three major, IDO1-inactive, circulating plasma metabolites were detected and characterized: M9, a direct O-glucuronide of EPA; M11, an amidine; and M12, N-dealkylated M11. Glucuronidation of EPA to form M9 is the dominant metabolic pathway, and in vitro, this metabolite is formed by UGT1A9. However, negligible quantities of M11 and M12 were detected when EPA was incubated with a panel of human microsomes from multiple tissues, hepatocytes, recombinant human cytochrome P450s (P450s), and non-P450 enzymatic systems. Given the reductive nature of M11 formation and the inability to define its source, the role of gut microbiota was investigated. Analysis of plasma from mice dosed with EPA following pretreatment with either antibiotic (ciprofloxacin) to inhibit gut bacteria or 1-aminobenzotriazole (ABT) to systemically inhibit P450s demonstrated that gut microbiota is responsible for the formation of M11. Incubations of EPA in human feces confirmed the role of gut bacteria in the formation of M11. Further, incubations of M11 with recombinant P450s showed that M12 is formed via N-dealkylation of M11 by CYP3A4, CYP2C19, and CYP1A2. Thus, in humans three major plasma metabolites of EPA were characterized: two primary metabolites, M9 and M11, formed directly from EPA via UGT1A9 and gut microbiota, respectively, and M12 formed as a secondary metabolite via P450s from M11.

Introduction

Epacadostat (EPA, INCB024360) is a first-in-class, orally active, investigational drug targeting the enzyme indoleamine 2,3-dioxygenase 1 (IDO1), which is activated in certain tumor tissues and acts as a key regulator of immunosuppressive mechanisms that are responsible for tumor escape from immune surveillance (Koblish et al., 2010; Liu et al., 2010). IDO1 is a heme-containing oxidoreductase that catalyzes the degradation of the essential amino acid tryptophan (Trp) to *N*-formyl-kynurenine (Kyn). Recent interest has focused on the role of IDO in the induction of tolerance to malignancy, as IDO-mediated oxidation of Trp results in a strong inhibitory effect on T cell–mediated responses by blocking T cell activation and inducing T cell apoptosis (Mellor et al., 2003). There have been clear demonstrations that an appropriately activated immune system can eradicate tumors in animal models (Finkelstein et al., 2004), and there is clinical evidence that manipulation of the immune system can be effective in a variety of human tumors, including malignant melanoma and lymphoma (Hsu et al., 1997; Dudley et al., 2002; Attia et al., 2005). Moreover, a Phase I/II study evaluating EPA in combination with pembrolizumab, an anti–programmed cell death protein 1 immunotherapeutic, indicated a 79% disease control rate in evaluable patients with advanced cancers (Gangadhar et al., 2015). Collectively, these data show that small-molecule inhibitors of IDO may provide a promising method to treat advanced malignancies in combination with chemotherapeutics and/or immunotherapy-based strategies.

Experiments to characterize the metabolism of new molecular entities (NMEs) are necessary for thorough consideration of drug safety and efficacy, as well as to evaluate the potential for drug-drug interactions. Although radiolabeled human absorption, distribution, metabolism, and excretion studies are considered definitive in the evaluation of an NME's metabolic fate, the use of samples from unlabeled clinical studies and synthesis of authentic metabolite standards can often achieve similar results in a timelier manner. Accordingly, the studies discussed herein were conducted to characterize the principal routes of EPA metabolism in humans prior to availability of radiolabeled human absorption, distribution, metabolism, and excretion results.

Material and Methods

Chemicals and Reagents

Pooled mixed-gender human hepatic microsomes, S9 fraction and cytosol, as well as recombinant human cytochrome P450 and UDP glucuronosyl transferase (UGT) Supersomes, were purchased from Corning Life Sciences (Tewksbury,

---

ABBREVIATIONS: ABT, 1-Aminobenzotriazole; AUC, area under the curve; DMSO, dimethylsulfoxide; EPA, epacadostat; ESMS, electrospray mass spectrometry; IDO1, indoleamine 2,3-dioxygenase; LC-MS/MS, liquid chromatography–tandem mass spectrometry; M9 (INCB056867), (Z)-6-((3-bromo-4-fluorophenylamino)(4-(2-(sulfamoylamino)ethylamino)-1,2,5-oxadiazol-3-yl)methyleneaminooxy)-3,4,5-trihydroxytetrahydro-2H-pyran-2-carboxylic acid; M11 (INCB056868), N-(3-bromo-4-fluorophenyl)-4-(2-(sulfamoylamino)ethylamino)-1,2,5-oxadiazole-3-carboximidamide; M12 (INCB052101), 4-amino-N-(3-bromo-4-fluorophenyl)-1,2,5-oxadiazole-3-carboximidamide; mARC, mitochondrial amidoxime–reducing component; MRM, multiple reaction monitoring; NME, new molecular entity; P450, cytochrome P450; UGT, uridine 5′-diphospho-glucuronyltransferase; UHP, ultra-high-performance.

MA). The UGT enzyme reaction solutions A (uridine diphosphate glucuronicacid) and B (buffer, magnesium chloride, and alamethicin) were also purchased from Corning Life Sciences. Pooled mixed-gender human intestinal, lung, and kidney microsomes and S9 fractions were purchased from Xenotech (Lenexa, KS). Pooled mixed-gender human liver homogenate and mitochondria were also purchased from Xenotech. Cryopreserved human hepatocytes were purchased from In Vitro ADMET Laboratories, LLC (Columbia, MD). Pooled fresh human feces homogenate (≥3 subjects) and pooled, fresh fasted CD-1 mouse feces homogenate were ordered from BioreclamationIVT (Westbury, NY). Pooled, fresh fasted Sprague Dawley rat feces was obtained in-house. Benzamidoxime and benzamidine were purchased from Sigma-Aldrich (St. Louis, MO). All commercially purchased reagents were either analytical or liquid chromatography–mass spectrometry grade.

Epacadostat (EPA, INCB024360, (Z)-N-(3-bromo-4-fluorophenyl)-N'-hydroxy-4-(2-(sulfamoylamino)ethylamino)-1,2,5-oxadiazole-3-carboximidamide) was synthesized by Incyte Corporation (Wilmington, DE) according to patent WO2006/122150 A2 applied for by Incyte Corporation: ^{1}H NMR (CD3CN, 500 MHz) δ: 9.06 (s, 1H), 7.47 (s, 1H), 7.22 (dd, J = 6.0, 2.7 Hz, 1H), 7.09 (dd, J = 8.7 Hz, 1H), 6.94 (ddd, J = 8.8, 4.1, 2.8 Hz, 1H), 6.06 (t, J = 5.6 Hz, 1H), 5.23 (t, J = 5.8 Hz, 1H), 5.18 (s, 2H), 3.47 (dt, J = 6.0,5.8 Hz, 2H), 3.26 (dt, J = 6.2,6.0 Hz, 2H); electrospray mass spectrometry (ESMS) m/z 438.0 [M+H]+.

M9 (INCB056867, (Z)-6-((3-bromo-4-fluorophenylamino)(4-(2-(sulfamoylamino) ethylamino)-1,2,5-oxadiazol-3-yl)methyleneaminooxy)-3,4,5-trihydroxytetrahydro-2H-pyran-2-carboxylic acid) was generated for Incyte Corporation by Hypha Discovery Ltd (Uxbridge, UK) using proprietary microbial biotransformation processes. The material was isolated as an off-white solid: ^{1}H NMR (CD3OD, 500 MHz): δ 7.24 (dd, J = 5.9, 2.5 Hz, 1H), 7.07 (dd, J = 8.6 Hz, 1H), 6.95–6.90 (m, 1H), 5.05 (d, J = 7.9 Hz, 1H), 3.83 (d, J = 9.0 Hz, 1H), 3.55–3.48 (m, 2H), 3.49–3.40 (m, 3H), 3.30–3.27 (m, 2H); ESMS m/z 614.0 [M+H]+. Additional structural confirmation was provided by: 1) the glucuronide anomeric proton at 5.05 ppm giving a long-range correlation to a ^{15}N with a chemical shift of –70.7 ppm relative to NH3, whereas the corresponding ^{15}N chemical shift in EPA is at –72.6 ppm; 2) the ^{15}N chemical shifts of the amino and sulfonamide nitrogens were significantly further upfield and showed no long-range correlations to any of the glucuronide protons.

M11 (INCB056868; N-(3-bromo-4-fluorophenyl)-4-(2-(sulfamoylamino) ethylamino)-1,2,5-oxadiazole-3-carboximidamide) was generated for Incyte Corporation by Hypha Discovery Ltd (Uxbridge, UK) using proprietary microbial biotransformation processes. The material was isolated as off-white solid; ^{1}H NMR (CD3CN, 500 MHz): δ 7.26 (dd, J = 6.5, 2.3 Hz, 1H), 7.23 (dd, J = 8.8, 8.9 Hz, 1H), 6.99 (ddd, J = 8.7, 4.4, 2.5 Hz, 1H), 6.80 (t, J = 5.6 Hz, 1H), 5.88 (s, 2H), 5.19 (t, J=5.8 Hz, 1H), 5.14 (s, 2H), 3.46 (dt, J = 6.1, 5.9 Hz, 2H), 3.25 (dt, J = 6.2, 5.9 Hz, 2H); ESMS m/z 422.0 [M+H]+.

M12 (INCB052101) (4-amino-N-(3-bromo-4-fluorophenyl)-1,2,5-oxadiazole-3-carboximidamide) was synthesized by Incyte Corporation (Wilmington, DE), from 4-amino-1,2,5-oxadiazole-3-carbonitrile and 3-bromo-4-fluoroaniline, by a procedure similar to that described in the literature (Koutentis and Mirallai, 2010). The material was isolated as a white solid; ^{1}H NMR (DMSO-d6, 400 MHz): δ 7.31 (dd, J = 8.8, 8.8 Hz, 1H), 7.26 (dd, J = 6.4, 2.5 Hz, 1H), 7.04 (s, 2H), 6.97 (ddd, J = 8.7, 4.5, 2.5 Hz, 1H), 6.59 (s, 2H); ESMS m/z 300.0 [M+H]+.

Clinical Study Designs

A clinical Phase I/II study was conducted in subjects with unresectable or metastatic melanoma to evaluate the safety and tolerability and dose-limiting toxicities of EPA administered in combination with ipilimumab and to evaluate the overall survival of subjects. This study was conducted in full accordance with ethical principles that have their origin in the Declaration of Helsinki and conducted in adherence to the study protocol, Good clinical practices as defined in Title 21 of the US Code of Federal Regulations (CFR) Parts 50, 54 56, 312, and Part 11, as well as International Conference on Harmonisation and good clinical practice consolidated guidelines (E6), applicable regulatory requirements, standard operating procedures for clinical investigation, and local laws regarding the protection of the rights and welfare of human participants in biomedical research. The protocols were approved by an independent institutional review board, and informed consent for all participants was obtained prior to screening. The study was composed of a Phase I dose escalation with multiple cohorts in which all subjects received ipilimumab (YERVOY, 3 mg/kg i.v. q 3 weeks) in combination with EPA and a Phase II study to evaluate overall survival of subjects

receiving ipilimumab (YERVOY, 3 mg/kg i.v. q 3 weeks) in combination with EPA. Blood samples for determination of plasma concentrations of EPA and metabolites were collected from the Phase I portion of the study on days 1 and 10. Plasma samples were analyzed for EPA and metabolites (M9, M11, and M12) using the clinical EPA liquid chromatography–tandem mass spectrometry (LC-MS/MS) method and the clinical metabolite LC-MS/MS method, both described below. The pharmacokinetic parameters for EPA and its metabolites were determined by standard noncompartmental methods using WinNonlin (version 6.0.0 or higher; Pharsight Corporation, Mountain View, CA).

Incubation of EPA with Individual Recombinant Human UGTs

EPA was incubated at a clinically relevant concentration (5 μM) at 37°C with recombinant human UGTs using microsomes prepared from baculovirus-infected insect cells transfected with cDNAs encoding human UGTs: UGT1A1, UGT1A3, UGT1A4, UGT1A6, UGT1A7, UGT1A8, UGT1A9, UGT1A10, UGT2B4, UGT2B7, UGT2B15, or UGT2B17. Each incubation contained 0.5 mg/ml of the individual isozyme, Tris-HCl buffer (50 mM, pH 7.5), magnesium chloride (8 mM), NADPH (1 mM), uridine diphosphate glucuronic acid (1 mM), alamethicin (25 μg/ml), and EPA [dissolved in dimethylsulfoxide (DMSO); 5 μM final substrate concentration and 0.1% final DMSO concentration]. Aliquots taken at 0, 15, 30, and 60 minutes were quenched with acetonitrile. After centrifugation, the supernatants were analyzed using the discovery LC-MS/MS method described below.

Incubation of EPA and M11 with Human Subcellular Fractions

EPA and M11 were incubated at a clinically relevant concentration (10 μM) at 37°C in pooled human microsomes and S9 fractions from liver, intestine, lung, and kidney with microsomal and S9 fraction protein concentrations of 2 mg/ml and 3 mg/ml, respectively. Additionally, EPA was incubated in pooled human liver cytosol with a cytosolic protein concentration of 5 mg/ml. Each incubation contained EPA or M11 (dissolved in DMSO; 10 μM final substrate concentration and 0.1% final DMSO concentration), potassium phosphate buffer (100 mM, pH 7.4), and NADPH (3 mM). Incubations were initiated with NADPH, and aliquots taken at 0 and 60 minutes were quenched with methanol. After centrifugation, the supernatants were analyzed using the semiquantitative biotransformation ultra-high-performance (UHP)LC-MS/MS method described below.

Incubation of EPA and M11 with Recombinant Human Cytochromes P450

EPA and M11 were incubated at a clinically relevant concentration (10 μM) at 37°C with individual human cytochrome P450 Supersomes™ (1A2, 2B6, 2C8, 2C19, 2D6, 3A4, 3A5, and 2C9). Each incubation contained 0.3 nmol/ml of the individual isozyme, NADPH (3 mM) and EPA or M11 (dissolved in DMSO; 10 μM final substrate concentration and 0.1% final DMSO concentration). All isozymes, except CYP2C9, were incubated in a potassium phosphate buffer solution (100 mM, pH 7.4). CYP2C9 incubations used Tris buffer (100 mM, pH 7.4). Incubations were initiated with NADPH and aliquots taken at 0 and 60 minutes were quenched with methanol. After centrifugation, the supernatants were analyzed using the semi-quantitative biotransformation UHPLC-MS/MS method described below.

Incubation of EPA and Benzamidoxime with Human Liver Homogenate and Subcellular Fractions

EPA and benzamidoxime (positive control) were incubated at a clinically relevant concentration (10 μM) at 37°C in pooled human liver homogenate and subcellular fractions (mitochondria, microsomes, S9 fraction, and cytosol). Each incubation contained 2 mg/ml protein, potassium phosphate buffer (100 mM, pH 6.0), NADH (2 mM), and EPA or benzamidoxime (dissolved in DMSO; 10 μM final substrate concentration and 0.1% final DMSO concentration). Incubations were initiated with NADH and aliquots taken at 0 and 30 minutes were quenched with 2 volumes of 1:1 (v/v) acetonitrile/methanol. After centrifugation, the supernatants were analyzed using the semiquantitative biotransformation UHPLC-MS/MS method for EPA or benzamidoxime described below.

Incubation of EPA and M9 with Human Feces with and without Antibiotics

Equal volumes of fresh human feces homogenate (1:4, w/v; phosphate-buffered saline) were shipped to Incyte under aerobic and anaerobic conditions,

TABLE 1

Area under the curve (AUC_{0-12h}) ratios of major EPA metabolites relative to EPA in humans following a single oral dose and at steady state.

Dose	Day	EPA	M9	M11	M12
50 mg BID	1	1	8.2	NC	NC
	10	1	8.1	0.3	0.8

NC, Not calculable because most plasma concentrations were below the lower limit of quantitation.

using a GasPak EZ Pouch System (Franklin Lakes, New Jersey) for shipment of the anaerobic fraction. Homogenates were incubated for 24 hours in a CO_2 incubator at 37°C, with the anaerobic fraction contained in a GasPak EZ Incubation Container with GasPak EZ Anaerobe Container System Sachets to provide an anaerobic environment. Aliquots of the resulting homogenates were transferred to individual vials for duplicate incubations with or without (control) antibiotics. Concentrations of antibiotics, EPA, and M9 used in these ex vivo incubations were roughly taken from clinically relevant doses divided by total human gut volume (1.65 l; Davies and Morris, 1993). Incubations were initiated with the addition of antibiotics [amoxicillin/clavulanate (Augmentin) and ciprofloxacin, 1mM] in phosphate-buffered saline (25% volume of incubation) then returned to the incubator under their respective aerobic and anaerobic conditions for 24 hours before addition of EPA or M9 dissolved in DMSO (100 μM final substrate concentration and 0.1% final DMSO concentration). The incubations were allowed to proceed for 24 hours, with aliquots taken at 0, 4 (EPA only), and 24 hours and stopped with 3 volumes of 1:1 (v/v) acetonitrile/methanol. After centrifugation, the supernatants were analyzed using the semiquantitative biotransformation UHPLC-MS/MS method described below.

Pharmacokinetics of EPA, M11, and M12 in Mice Given EPA following Antibiotic or 1-Aminobenzotriazole Pretreatment

This pharmacokinetic study was conducted in accordance with guidelines from the Institutional Animal Care and Use Committee. Three groups of male CD-1 mice were pretreated with either: 1) 6 days of QD PO ciprofloxacin (10 mg/kg in 0.5% methylcellulose), 2) two PO doses of 1-aminobenzotriazole (ABT; 50 mg/kg in 0.5% methylcellulose) 18 and 2 hours before EPA administration, or 3) no treatment (control). EPA was administered on day 6 as a single 100-mg/kg oral dose (5% dimethylacetamide in 0.5% methylcellulose). Terminal blood samples were collected at 0, 1.5, 4, 6, and 24 hours postdose (three mice per time point). Plasma samples were precipitated with acetonitrile containing internal standard. After centrifugation, the supernatants were analyzed using the quantitative biotransformation UHPLC-MS/MS method described below. The pharmacokinetic parameters for EPA and its metabolites were determined by standard
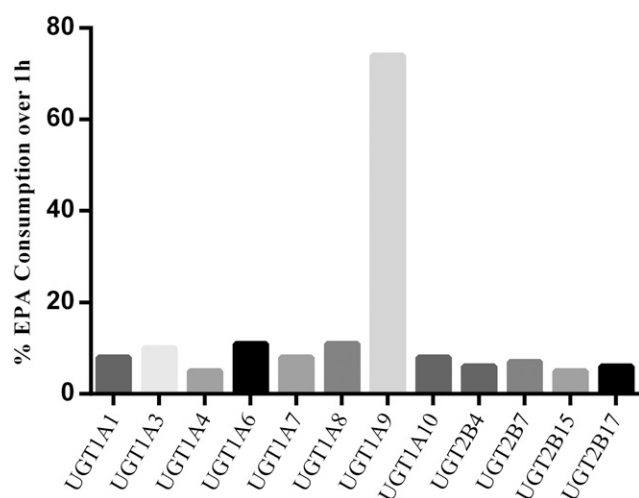
noncompartmental methods using WinNonlin (version 6.0.0 or higher; Pharsight Corporation, Mountain View, CA).

LC-MS/MS Analysis

Clinical LC-MS/MS Methods. For EPA quantitation, plasma samples were analyzed by a validated, good laboratory practice, LC-MS/MS method at Incyte Corporation. Plasma concentrations were determined following a liquid/liquid extraction procedure with internal standard. Chromatography was performed with an ACE 3 C8 HPLC column (50 × 2.1 mm, 3 μm; Advanced Chromatography Technologies, Aberdeen, Scotland) at ambient temperature under isocratic conditions and a mobile phase consisting of 48% acetonitrile and 52% 2 mM ammonium formate, pH 3, aqueous solution at a flow rate of 350 μl/min. LC-MS/MS analysis was performed using a positive TurboIonSpray interface on a Sciex API-3000 operating in positive ionization mode with multiple reaction monitoring (MRM) transition, m/z 438.0 → 359.0. EPA and internal standard chromatographic peaks were acquired and integrated using Analyst software (version 1.4.1; Thermo Fisher Scientific, Sunnyvale, CA). Peak areas were imported into Watson LIMS (version 7.4.1; Thermo Fisher Scientific, Waltham, MA) for quantitative analysis.

M9, M11, and M12 plasma concentrations were determined in a non-good laboratory practice setting with nonvalidated methods using protein precipitation with acetonitrile/methanol, 90:10, and an internal standard. Chromatography was performed with an ACE 3 C8 HPLC column (2.1 × 50 mm, 3 μm; Advanced Chromatography Technologies) at ambient temperature with a gradient composed of water with 0.1% formic acid (mobile phase A) and acetonitrile with 0.1% formic acid (mobile phase B) at a flow rate of 300 μl/min. Gradient conditions with linear increases of mobile phase B were as follows: 0 minutes, 20% B; 1 minute, 20% B; 3.5 minutes, 85% B; 4.0 minutes, 85% B; 4.1 minutes, 20% B; 4.5 minutes, stop. LC-MS/MS analysis was performed using a TurboIonSpray interface on a Sciex API-4000 operating in positive ionization mode with MRM transitions: M9 (m/z 614.2 → 438.0), M11 (m/z 422.2 → 343.2) and M12 (m/z 300.1 → 283.0). Chromatographic peaks were integrated and quantitative analysis was performed using Analyst software (version 1.4.1).

Discovery LC-MS/MS Method. Supernatants were analyzed using a Sciex 3000 mass spectrometer (Applied Biosystems/MDS SCIEX, Foster City, CA) coupled to a Shimadzu SCL-10A controller with a Shimadzu LC-10A binary gradient pump system (Shimadzu Scientific Instruments, Columbia, MD) and a HTC PAL autosampler (CTC Analytics AG, Zwingen, Switzerland). Chromatographic separation was achieved using a Synergi Hydro-RP HPLC column (2.0 × 30 mm, 4 μm; Phenomenex Inc., Torrance, CA) and a gradient elution scheme consisting of mobile phase A (0.1% formic acid in water) and mobile phase B
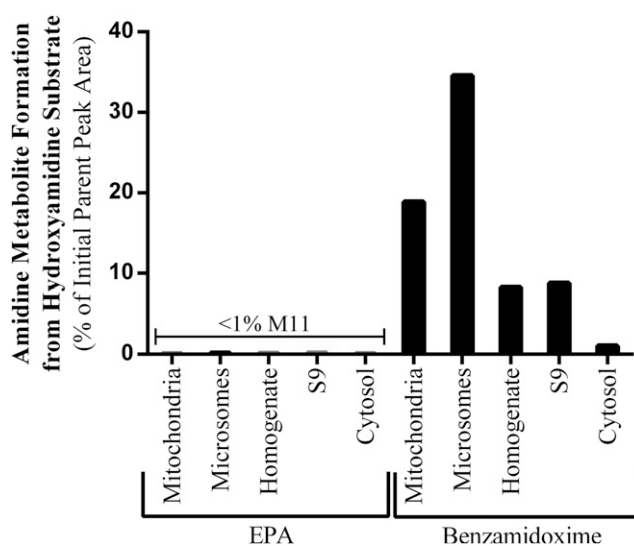

Fig. 1. In vitro consumption of EPA (5 μM) by individual recombinant human UGTs (0.5 mg/ml) over 1 hour.

Fig. 2. Formation of M11 from EPA (10 μM) and benzamidine from benzamidoxime (10 μM) by human liver mitochondria, microsomes, homogenate, S9 fraction and cytosol (2 mg/ml protein) over 30 minutes. Incubations were conducted in potassium phosphate buffer (pH 6.0) with NADH (2 mM).

(0.1% formic acid in acetonitrile), in which mobile phase B was held at 10% for 0.5 minutes, then increased linearly from 10% to 90% over 1 minute and held at 90% for 0.5 minutes before being returned to 10% at a flow rate of 0.45 ml/min. MRM analysis for EPA was performed in the positive ionization mode, using the mass transition m/z 438 → 359. Chromatographic peaks were integrated using Analyst software (version 1.4.1).

Biotransformation UHPLC-MS/MS Method. Samples were assayed using a Q Exactive Orbitrap LC-MS/MS system coupled to a Dionex Ultimate 3000 UHPLC System (Thermo Fisher Scientific, Waltham, MA). Separation of EPA and its metabolites was achieved using a Supelco Titan C18 UHPLC column (3 × 100 mm, 1.9 μm; Sigma-Aldrich) or an ACE Excel SuperC18 UHPLC column (2.1 × 150 mm, 2 μm) with a gradient composed of 3 mM ammonium formate with 0.1% formic acid (mobile phase A) and acetonitrile (mobile phase B) that increased linearly from 10% to 100% B over 10 minutes at a flow rate of 500 μl/min. Separation of benzamidoxime and benzamidine was achieved using a Phenomenex Kinetex Biphenyl UHPLC column (2.1 × 150 mm, 1.7 μm; Phenomenex Inc.) with a gradient composed of 3 mM ammonium formate with 0.1% formic acid in (mobile phase A) and acetonitrile (mobile phase B) that increased linearly from 5 to 95% B over 10 minutes at a flow rate of 400 μl/min. Semiquantitative analysis was performed using positive electrospray ionization with full MS with or without data-dependent MS2. Quantitative analysis of preclinical samples was performed using positive electrospray ionization with targeted MS2 for the parent ions of interest and a prominent daughter ion thereof: EPA (m/z 438.00 → 359.02619), M9 (m/z 614.03 → 437.99899), M11 (m/z 422.00 → 343.03128), and M12 (m/z 299.99 → 282.96253). Chromatographic peaks were integrated and analyte concentrations calculated using Xcalibur software (version 2.2, SP1; Thermo Fisher Scientific).

Results

M9, M11, and M12 are Major Metabolites of EPA in Humans

Three abundant plasma metabolites of EPA were first detected in preclinical species: M9 (INCB056867), a direct O-glucuronide of EPA; M11 (INCB056868), an amidine; and M12 (INCB052101), an N-dealkylated amidine (Fig. 5). Synthetic standards were then prepared to fully characterize these compounds, including quantification in plasma from human subjects with pharmacokinetic analysis. All three metabolites were found to be IDO-1 inactive (human IDO inhibitory IC$_{50}$ values > 20 μM). The ratios of exposure are shown in Table 1, on the basis of area under the curve (AUC) of EPA, M9, M11, and M12 after a single dose and at steady state in humans given 50 mg BID. M9, the direct glucuronide metabolite of EPA, was the most abundant metabolite detected, with a mean AUC value that was more than 8-fold greater than that of EPA following a single dose and at steady state. M11 and M12 were detected at levels that were 30 and 80% that of EPA at steady state. However, M11 and M12 were not detected after a single dose, presumably because the 12-hour timeframe was not sufficient for M11 to be formed by the gut microbiota and absorbed from the intestine. It is interesting to note that at steady state at a higher dose (300 mg BID), the ratios of M11 and M12 to EPA were higher, at 2.5 and 3.0, respectively, whereas M9 remained at 7.0 (data not shown). These results affirm that all three metabolites are considered major by FDA and International Conference on Harmonisation guidelines.

UGT1A9 Is Responsible for Glucuronidation of EPA

Because glucuronidation was identified to be a major route of in vivo EPA metabolism, in vitro assays were conducted with recombinant human glucuronosyltransferases (UGTs). EPA was extensively metabolized by only UGT1A9, with 74% of the initial concentration of EPA consumed over the 60-minute incubation (Fig. 1). This UGT1A9 incubation was analyzed by LC-MS/MS to monitor glucuronide metabolites; a single peak was detected corresponding to M9 (m/z 614). The recombinant enzyme preparations of UGT1A1, UGT1A3, UGT1A4, UGT1A6, UGT1A7, UGT1A8, UGT1A10, UGT2B4, UGT2B7, UGT2B15, or

UGT2B17 isozymes showed little to no EPA turnover (within experimental error).

M11 Is Not Formed by Human Tissue Subcellular Fractions

EPA was not metabolized to M11 or M12 (≤1% of integrated EPA peak area) by human hepatocytes or microsomes and S9 fractions prepared from liver, intestine, lung, or kidney. Moreover, individual human P450s, CYPs 1A2, 2B6, 2C8, 2C19, 2D6, 3A4, 3A5, and 2C9, did not form M11 or M12 from EPA (≤1% of integrated EPA peak area). Finally, EPA was stable in human liver homogenate and subcellular fractions (mitochondria, microsomes, S9 fraction, and cytosol) when incubated under conditions promoting the activity of mitochondrial amidoxime–reducing component (mARC) proteins (Jakobs et al., 2014; Ott et al., 2015), and benzamidoxime, the control substrate for mARC-catalyzed hydroxyamidine reduction, was readily reduced to benzamidine (Fig. 2).

M11 Is Formed by Gut Microbiota

When EPA was incubated with human feces homogenate under aerobic and anaerobic conditions over 24 hours, M11 was detected at levels comparable to parent at the end of the incubation (139% and 100% of integrated EPA peak area at 24 hours, respectively), whereas M12 was detected in trace quantities only. Similarly, when EPA was incubated with mouse and rat feces homogenates, M11 was detected at levels that ranged from 12 to 30% of the integrated EPA peak area at 24 hours (data on file at Incyte). Even though 99% of colonic microbiota are reported to be anaerobic (McCabe et al., 2015), M11 was formed to similar extents
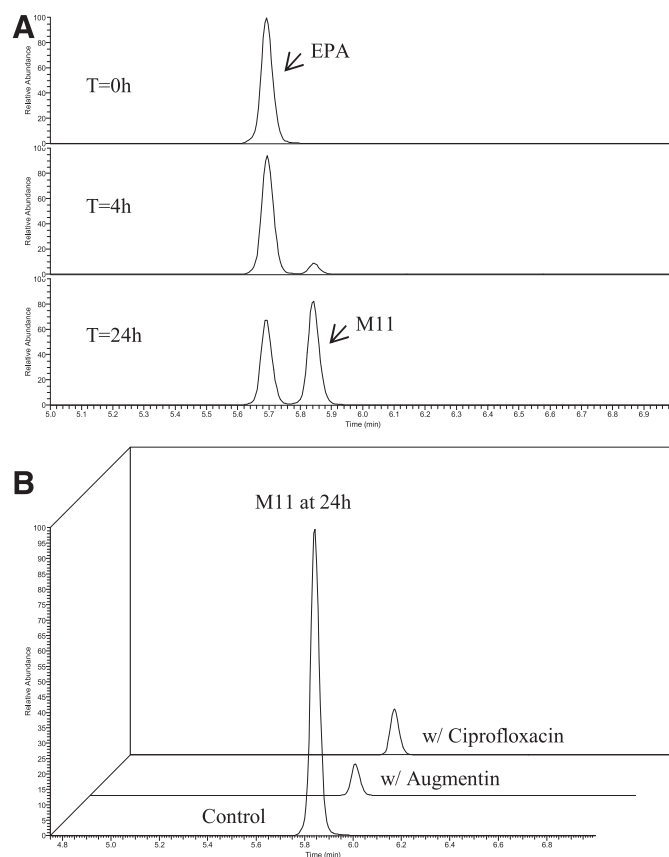
Fig. 3. Representative extracted ion chromatograms showing ex vivo formation of M11 from EPA in human feces homogenate (a) and decrease in M11 formation from EPA in human feces homogenate by commonly prescribed antibiotics (b).

under both aerobic and anaerobic conditions. Figure 3a shows a representative chromatogram of EPA conversion to M11 under aerobic conditions. Addition of antibiotics amoxicillin/clavulanate (Augmentin) and ciprofloxacin to the fecal incubations under aerobic conditions decreased M11 formation by 91% and 94%, respectively (Fig. 3b).

M9 Is Deconjugated to EPA by Gut Microbiota

In addition to EPA, the glucuronide metabolite M9 was incubated in human feces, as glucuronides are known to participate in enterohepatic recirculation (i.e., absorption of parent, conjugation in the liver, excretion into the bile, and then into the small intestine, deconjugation back to parent in the intestine, and reabsorption as parent). When M9 was incubated with human feces homogenate under aerobic and anaerobic conditions, virtually 100% of M9 was consumed in 24 hours (2.3% and 0.0% of M9 remaining, respectively, on the basis of integrated peak area). The only major drug-related products observed in these M9 feces incubations were EPA and M11, accounting for 77–81% and 19–23% of observed turnover, respectively (data on file at Incyte). The M11 formed in these incubations of M9 in feces is thought to be via initial deglucuronidation of M9 to form EPA with subsequent reduction of EPA to form M11.

Formation of M11 in Mice Given EPA following Antibiotic or ABT Pretreatment

Analysis of plasma from mice dosed orally with EPA following antibiotic (ciprofloxacin) pretreatment to inhibit metabolism by gut microbiota (Table 2) showed a 46% decrease in M11 formation relative to control animals (M11/EPA AUC ratios of 0.119 versus 0.260, respectively), supporting M11 formation by the gut microbiome. In contrast, pretreatment with ABT to inhibit cytochrome P450 metabolism did not show a decrease in M11 formation relative to control animals, corroborating the lack of M11 formation in microsomal and recombinant P450 incubations. In fact, the M11/EPA AUC ratio for the ABT pretreatment group was 0.372, an increase from control (M11/EPA AUC ratio 0.260). This increase probably resulted from inhibition of the M11 clearance pathway via P450s (see below).

M12 Is a Secondary Metabolite of EPA Formed from M11. Metabolite M12 was not detected in vitro when EPA was incubated with human microsomes, S9 fractions, or recombinant P450s. Additionally, M12 was formed in trace quantities at most in ex vivo human, mouse, and rat feces homogenates (vide supra). However, Fig. 4 shows that M12 was formed when M11 was incubated in human liver microsomes and S9 fraction (1.5–4.8% M11 parent peak area). Further, incubations of M11 with individual recombinant human P450s showed that CYPs 3A4, 2C19, and 1A2 catalyze the N-dealkylation of M11 to form M12. These incubations also demonstrated that CYP3A4 is primarily responsible for the metabolism of M11 (>90% consumed in the incubation), with M12 as the most abundant metabolite detected. Finally, as shown in Table 2, plasma analysis of mice dosed orally with EPA immediately following pretreatment with ABT to inhibit cytochrome P450 metabolism clearly showed a decrease in M12 relative to control animals. Comparison of the AUC ratio of M12 with M11 shows that M12 formation was diminished following pretreatment with ABT versus control (M12/M11 AUC ratios of 0.045 versus 0.411), whereas the ratio was similar between antibiotic pretreatment and control (M12/M11 AUC ratios of 0.372 versus 0.411). These results confirm M12 is a secondary metabolite of M11.

Discussion

It was recently reported that, of the 35 NMEs approved by FDA in 2014, the metabolism of 32 NMEs was well characterized using the standard complement of human liver subcellular fractions, hepatocytes, and recombinant enzymes. The majority of this subset of 32 NMEs is metabolized primarily by cytochrome P450 enzymes, though Phase II metabolism by UGTs and sulfotransferases did contribute in several instances (Yu, et al., 2016). This is not unexpected as, by design, most drugs are rapidly and effectively absorbed in the small intestine and subjected to first-pass and systemic metabolism. However, a drug that is not absorbed continues through the gastrointestinal tract where it can undergo metabolism by gut bacteria, primarily in the large intestine (Sousa, et al., 2008). In contrast to the oxidative and conjugative metabolism favored following systemic absorption, metabolism by gut bacteria is mostly reductive and hydrolytic (Testa, 1995; Sousa, et al., 2008; Klaassen and Cui, 2015). During investigation of the metabolism of EPA, it became evident that EPA is an unusual case in which major circulating metabolites stem from extensive Phase II metabolism, reductive metabolism by gut microbiota, and secondary systemic Phase I metabolism of the absorbed gut metabolite.

The metabolic fate of EPA was initially characterized in preclinical species, which identified M9 (INCB056867), a direct O-glucuronide of EPA; M11 (INCB056868), an amidine; and M12 (INCB052101), N-dealkylated M11. Because of the steady-state exposure of these circulating metabolites in humans (vide infra) and the implications in the design of future clinical drug-drug interaction studies with EPA, full characterization of each was necessary, including sourcing of metabolite
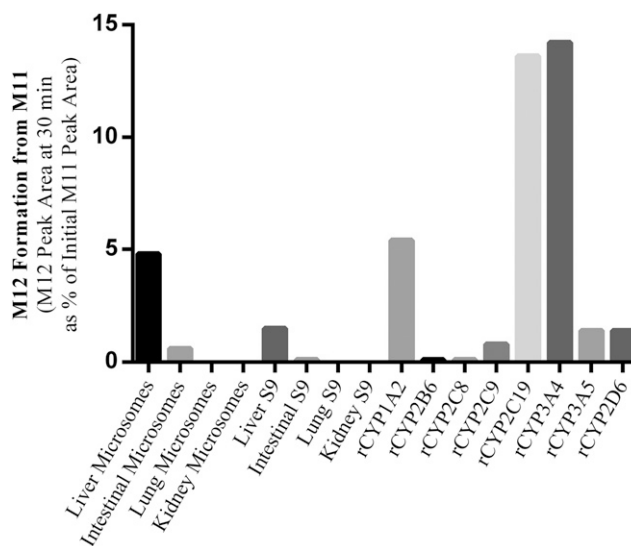
TABLE 2

In vivo formation of M11 and M12 in mice given EPA with and without antibiotic or ABT pretreatment.

Dose Group	AUC$_{0-6h}$ Ratio Relative to EPA		
	EPA	M11	M12
Control	1.000	0.260	0.107
Ciprofloxacin pretreatment	1.000	0.119	0.044
ABT pretreatment	1.000	0.372	0.017
AUC$_{0-6h}$ ratio relative to M11			
Control		1.000	0.411
Ciprofloxacin pretreatment		1.000	0.372
ABT pretreatment		1.000	0.045

Fig. 4. Formation of M12 from M11 (10 μM) by human tissue microsomes (2 mg/ml protein) and S9 fractions (3 mg/ml protein) and recombinant cytochrome P450s (0.3 nmol/ml).

generation. Accordingly, multiple in vitro experiments were conducted to identify the specific UGT isozymes responsible for the direct glucuronidation of EPA and the Phase I enzymes and/or the physiologic site responsible for the reduction of EPA to M11 and oxidation to M12. Because of the multifaceted nature of EPA metabolism, vis-à-vis glucuronidation, reduction, and oxidation, and because the extent of EPA reduction to M11 is beyond the norm of xenobiotic-metabolizing enzymes, metabolism of EPA by atypical systems/sites (e.g., gut microbiome and mitochondria) was explored.

M9, the direct O-glucuronic acid conjugate of the amidoxime in EPA, was the most abundant circulating metabolite detected in humans following a single dose and at steady state, with AUC values approximately 8-fold greater than that of parent EPA. In vitro studies of EPA with recombinant UGT isoforms identified UGT1A9 as the principal isoform responsible for the formation of M9. Although UGT1A9 represents 6.1% of total UGT expression in hepatic tissue (Ye et al., 2014), it is one of the more prominent hepatic UGTs involved in the metabolism of NMEs (Yu et al., 2016). UGTs are a superfamily of isoforms known to have distinct, but overlapping, substrate selectivities, yet the underlying mechanism governing the observed selectivity is not completely understood (Radominska-Pandya, et al., 1999; Sorich, et al., 2004; Miners, et al., 2010; Wu et al., 2012). Generally, UGT1A9 has been shown to prefer sterically hindered nucleophiles bound to an aromatic ring (e.g., propofol; Lee et al., 2003; Sorich et al., 2004; Xia et al., 2014), though this does not fit the chemical structure of EPA. Additionally, UGT1A9 is known to glucuronidate N-hydroxylated arylamines and by extension was found to be the major isoform responsible for O-glucuronidation of benzamidoxime (Fröhlich et al., 2005). Benzamidoxime is a model substrate for studying the metabolism of N-hydroxyamidines, the same functional group that is glucuronidated in EPA to form M9. Interestingly, benzamidoxime and other hydroxy-amidines are also reduced to the corresponding amidine in micro-somal fractions and mitochondrial preparations (Clement, 2002); no such reduction of EPA has been observed in vitro, even though the amidoxime reduction metabolite (M11) is a major in vivo circulating metabolite.

At steady state in humans, the AUC value for M11 was 30% of parent EPA. M11 is a Phase I metabolite of EPA, wherein the amidoxime (N-hydroxyamidine) is reduced to the amidine. Reduction reactions by typically evaluated xenobiotic metabolizing enzymes (e.g., P450s), although not rare, are not commonplace (Testa, 1995). Illustrating this point, M11 was not formed by human microsomes or S9 fractions from multiple tissues, including liver. Moreover, M11 was not formed by human hepatocytes or recombinant P450s. Finally, drawing upon the reductive nature of M11 formation and the recent characterization of mARC proteins (Jakobs et al., 2014; Ott et al., 2015), human liver homogenate, microsomes, S9 fraction, mitochondria, and cytosol were tested for M11 formation from EPA, under conditions to promote mARC activity, without success. Given that M11 is formed via reduction of EPA and with no success in generating M11 in vitro across any commonly used metabolic system, we suspected this metabolite was formed via gut microbiota, as bacteria can be responsible for reductive and hydrolytic metabolism. Although there is a renewed interest in the metabolic capabilities of gut microbiota, only ~1% of the approved drugs are known to be substrates of gut microbiota (Yip and Chan, 2015). The colon is the primary source of microbial colonization in humans (Hao and Lee, 2004) and, consequently, the site of most xenobiotic metabolism in the gut (Klaassen and Cui, 2015). After incubating EPA with human feces under aerobic and anaerobic conditions, substantial levels of M11 were formed, and when antibiotics were included in the incubations, M11 formation was diminished by up to 94%. Furthermore, when mice were pretreated with the antibiotic ciprofloxacin by mouth and then given EPA orally, M11 formation was reduced by half versus control mice that were not pretreated with ciprofloxacin, corroborating the ex vivo observation that M11 is formed by bacteria in feces. In line with these results, pretreatment of mice with ABT, a pan-P450 inhibitor, did not reduce M11 formation from EPA versus control mice. ABT did, however, reduce the formation of M12, the putative N-dealkylated metabolite of M11, to 15% of control levels. Additional in vitro studies showed that M11 undergoes P450-mediated conversion to M12. In humans, as with M11, the AUC value of M12 was 80% of EPA at steady state, reflective of the formation of M12 via P450-mediated N-dealkylation of M11. In total, these data suggest that unabsorbed EPA or EPA in the intestine potentially via enterohepatic recirculation is converted to M11 by gut microbiota, with M11 then absorbed and metabolized to M12 in the liver. It is worth noting that
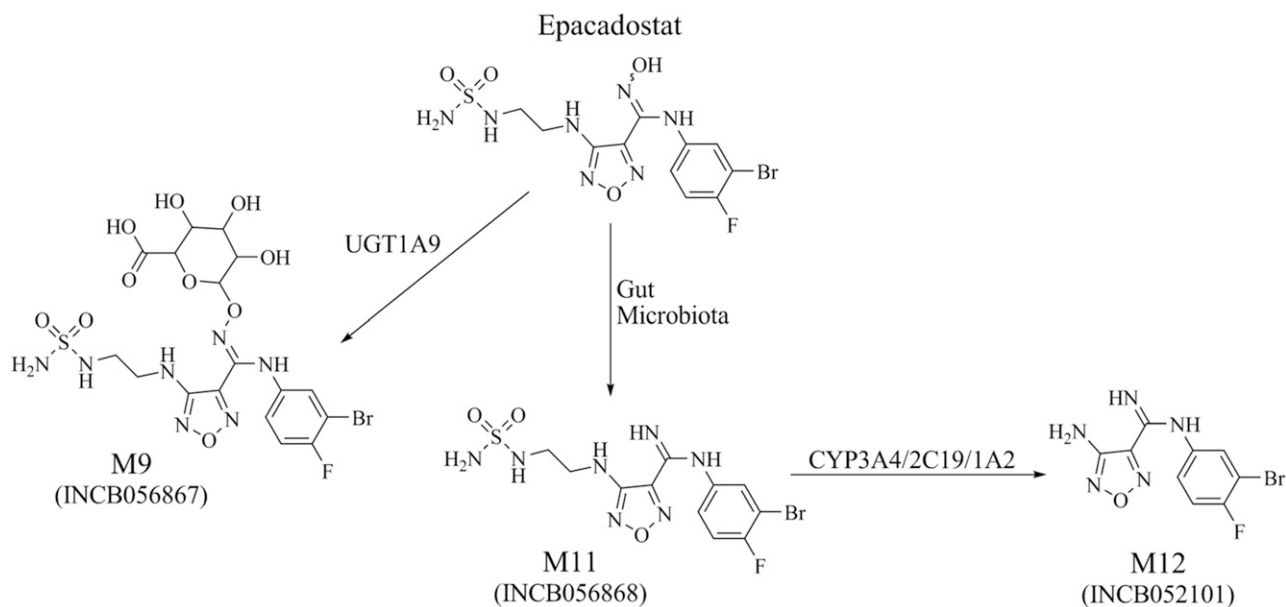
Fig. 5. Proposed major metabolic pathways of EPA in humans.

N-hydroxylation of amidines in liver homogenates has been shown (Clement et al., 1994; Fröhlich, et al., 2005), but no such oxidation of M11 back to EPA has been observed, nor has initial N-dealkylation of EPA to form the corresponding N-hydroxyamidine of M12, prior to reduction to M12.

EPA is a promising first-in-class, orally active, investigational drug targeting the enzyme IDO1. The results presented herein elucidate the metabolism of EPA to three major human metabolites involving Phase II metabolism (glucuronidation), reductive metabolism by gut microbiota, and secondary systemic Phase I metabolism of the absorbed gut metabolite (Fig. 5).

Authorship Contributions

Participated in research design: Boer, Bowman, Yang, Combs, Yeleswaram, Diamond.

Conducted experiments: Boer, Young-Sciame, Lee, Bowman, Nedza, Galya, Frietze.

Contributed new reagents or analytic tools: Frietze, Combs.

Performed data analysis: Boer, Bowman, Yang, Shi, Galya, Frietze, Yeleswaram, Diamond.

Wrote or contributed to the writing of the manuscript: Boer, Yeleswaram, Diamond.

References

Attia P, Phan GQ, Maker AV, Robinson MR, Quezado MM, Yang JC, Sherry RM, Topalian SL, Kammula US, Royal RE, et al. (2005) Autoimmunity correlates with tumor regression in patients with metastatic melanoma treated with anti-cytotoxic T-lymphocyte antigen-4. *J Clin Oncol* **23**: 6043–6053.

Clement B (2002) Reduction of N-hydroxylated compounds: amidoximes (N-hydroxyamidines) as pro-drugs of amidines. *Drug Metab Rev* **34**:565–579.

Clement B, Schultze-Mosgau MH, Richter PH, and Besch A (1994) Cytochrome P450-dependent N-hydroxylation of an aminoguanidine (amidinohydrazone) and microsomal retroreduction of the N-hydroxylated product. *Xenobiotica* **24**:671–688.

Davies B and Morris T (1993) Physiological parameters in laboratory animals and humans. *Pharm Res* **10**:1093–1095.

Dudley ME, Wunderlich JR, Robbins PF, Yang JC, Hwu P, Schwartzentruber DJ, Topalian SL, Sherry R, Restifo NP, Hubicki AM, et al. (2002) Cancer regression and autoimmunity in patients after clonal repopulation with antitumor lymphocytes. *Science* **298**:850–854.

Finkelstein SE, Heimann DM, Klebanoff CA, Antony PA, Gattinoni L, Hinrichs CS, Hwang LN, Palmer DC, Spiess PJ, Surman DR, et al. (2004) Bedside to bench and back again: how animal models are guiding the development of new immunotherapies for cancer. *J Leukoc Biol* **76**: 333–337.

Fröhlich AK, Girreser U, and Clement B (2005) Metabolism of benzamidoxime (N-hydroxyamidine) in human hepatocytes and role of UDP-glucuronosyltransferases. *Xenobiotica* **35**:17–25.

Gangadhar TC, Hamid O, Smith DC, Bauer TM, Wasser JS, Luke JJ, Balmanoukian AS, Kaufman DR, Zhao Y, Maleski J et al. (2015) Preliminary results from a Phase I/II study of epacadostat (INCB024360) in combination with pembrolizumab in patients with selected advanced cancers, oral presentation at: 30th Annual Meeting and Associated Programs of the Society for Immunotherapy of Cancer (SITC); 2015 Nov 4; National Harbor, MD. Society for Immunotherapy of Cancer, Milwaukee, WI.

Hao WL and Lee YK (2004) Microflora of the gastrointestinal tract: a review. *Methods Mol Biol* **268**:491–502.

Hsu FJ, Caspar CB, Czerwinski D, Kwak LW, Liles TM, Syrengelas A, Taidi-Laskowski B, and Levy R (1997) Tumor-specific idiotype vaccines in the treatment of patients with B-cell lymphoma–long-term results of a clinical trial. *Blood* **89**:3129–3135.

Jakobs HH, Froriep D, Havemeyer A, Mendel RR, Bittner F, and Clement B (2014) The mitochondrial amidoxime reducing component (mARC): involvement in metabolic reduction of N-oxides, oximes and N-hydroxyamidinohydrazones. *ChemMedChem* **9**:2381–2387.

Klaassen CD and Cui JY (2015) Review: Mechanisms of How the Intestinal Microbiota Alters the Effects of Drugs and Bile Acids. *Drug Metab Dispos* **43**:1505–1521.

Koblish HK, Hansbury MJ, Bowman KJ, Yang G, Neilan CL, Haley PJ, Burn TC, Waeltz P, Sparks RB, Yue EW, et al. (2010) Hydroxyamidine inhibitors of indoleamine-2,3-dioxygenase potently suppress systemic tryptophan catabolism and the growth of IDO-expressing tumors. *Mol Cancer Ther* **9**:489–498.

Koutentis PA and Mirallai SI (2010) Reinvestigating the synthesis of N-arylbenzamidines from benzonitriles and anilines in the presence of AlCl3. *Tetrahedron* **66**:5134–5139.

Lee J, Obach RS, and Fisher M (2003) *Drug Metabolizing Enzymes: Cytochrome P450 and Other Enzymes in Drug Discovery and Development*, Marcel Dekker Inc., New York.

Liu X, Shin N, Koblish HK, Yang G, Wang Q, Wang K, Leffet L, Hansbury MJ, Thomas B, Rupar M, et al. (2010) Selective inhibition of IDO1 effectively regulates mediators of antitumor immunity. *Blood* **115**:3520–3530.

McCabe M, Sane RS, Keith-Luzzi M, Xu J, King I, Whitcher-Johnstone A, Johnstone N, Tweedie DJ, and Li Y (2015) Defining the Role of Gut Bacteria in the Metabolism of Deleobuvir: In Vitro and In Vivo Studies. *Drug Metab Dispos* **43**:1612–1618.

Mellor AL, Baban B, Chandler P, Marshall B, Jhaver K, Hansen A, Koni PA, Iwashima M, and Munn DH (2003) Cutting edge: induced indoleamine 2,3 dioxygenase expression in dendritic cell subsets suppresses T cell clonal expansion. *J Immunol* **171**:1652–1655.

Miners JO, Mackenzie PI, and Knights KM (2010) The prediction of drug-glucuronidation parameters in humans: UDP-glucuronosyltransferase enzyme-selective substrate and inhibitor probes for reaction phenotyping and in vitro-in vivo extrapolation of drug clearance and drug-drug interaction potential. *Drug Metab Rev* **42**:196–208.

Ott G, Havemeyer A, and Clement B (2015) The mammalian molybdenum enzymes of mARC. *J Biol Inorg Chem* **20**:265–275.

Radominska-Pandya A, Czernik PJ, Little JM, Battaglia E, and Mackenzie PI (1999) Structural and functional studies of UDP-glucuronosyltransferases. *Drug Metab Rev* **31**:817–899.

Sorich MJ, Miners JO, McKinnon RA, and Smith PA (2004) Multiple pharmacophores for the investigation of human UDP-glucuronosyltransferase isoform substrate selectivity. *Mol Pharmacol* **65**:301–308.

Sousa T, Paterson R, Moore V, Carlsson A, Abrahamsson B, and Basit AW (2008) The gastrointestinal microbiota as a site for the biotransformation of drugs. *Int J Pharm* **363**:1–25.

Testa B (1995) *The Metabolism of Drugs and Other Xenobiotics: Biochemistry of Redox Reactions*, Academic Press, London, UK.

Wu B, Wang X, Zhang S, and Hu M (2012) Accurate prediction of glucuronidation of structurally diverse phenolics by human UGT1A9 using combined experimental and in silico approaches. *Pharm Res* **29**:1544–1561.

Xia YL, Liang SC, Zhu LL, Ge GB, He GY, Ning J, Lv X, Ma XC, Yang L, and Yang SL (2014) Identification and characterization of human UDP-glucuronosyltransferases responsible for the glucuronidation of fraxetin. *Drug Metab Pharmacokinet* **29**:135–140.

Ye L, Yang X, Guo E, Chen W, Lu L, Wang Y, Peng X, Yan T, Zhou F, and Liu Z (2014) Sorafenib metabolism is significantly altered in the liver tumor tissue of hepatocellular carcinoma patient. *PLoS One* **9**:e96664.

Yip LY and Chan ECY (2015) Investigation of host-gut microbiota modulation of therapeutic outcome. *Drug Metab Dispos* **43**:1619–1631.

Yu J, Ritchie TK, Zhou Z, and Ragueneau-Majlessi I (2016) Key findings from preclinical and clinical drug interaction studies presented in new drug and biological license applications approved by the Food and Drug Administration in 2014. *Drug Metab Dispos* **44**:83–101.

Address correspondence to: Dr. Jason Boer, Incyte Corporation, 1801 Augustine Cut-Off, Wilmington, DE 19803. E-mail: jboer@incyte.com